

MOST Project-4

USRL RESEARCH REPORT, No. 57
15 November 1961

AD A 044 708

INTERFERENCE VERSUS FREQUENCY IN MEASUREMENTS
IN A SHALLOW LAKE.

Robert J. Bobber

22 Mar 64

USRL-RR-57

DDC

SEP 23 1977

Note in file: Valueless?

Reprinted from the Journal of the Acoustical Society of America
Vol. 33, No. 9, pages 1211-1215, September 1961

Department of the Navy

Office of Naval Research

UNDERWATER SOUND REFERENCE LABORATORY

P. O. Box 8337

Orlando, Florida

254 300

LB



Interference Versus Frequency in Measurements in a Shallow Lake

ROBERT J. BOEDER

U. S. Navy Underwater Sound Reference Laboratory, Orlando, Florida

(Received March 22, 1961)

When an omnidirectional projector and hydrophone are closely spaced and in shallow water, and sound is transmitted from one to the other, a large interference signal is superimposed on the direct signal. If the received signal is plotted as a function of frequency, as in a calibration measurement, the interference signal amplitude appears to be an inconsistent series of irregular sharp peaks and dips. A mathematical analysis of the condition where the transducers are midway between a water-air surface and a bubble covered bottom shows that the shape, amplitude, and frequency of the interference pattern are predictable as the result of a large number of multireflection paths.

INTRODUCTION

ACOUSTICAL measurements, particularly for the calibration of underwater sound transducers, are often made in shallow water. For economic or other practical reasons the absence of good free field conditions must be tolerated.

The Underwater Sound Reference Laboratory calibrates transducers in a lake 25 to 30 ft deep. This depth is ample for measurements at ultrasonic frequencies because measurement transducers can be made directional to avoid difficulties with reflections from the top and bottom boundaries. Surface-reflected sound in the direction of minor lobes of the radiation pattern, and other types of interference, are easily recognized and accounted for. For example, Fig. 1 is a trace of a hydrophone output voltage versus frequency. The solid line is the measured voltage. The dashed line is the corrected voltage. The oscillating pattern can be identified as surface reflection interference from¹

$$\Delta f = c / \Delta d, \quad (1)$$

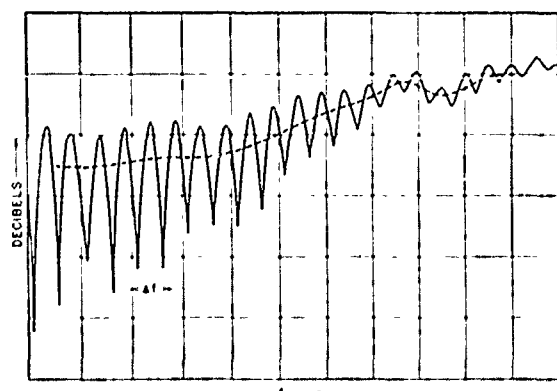


FIG. 1. Measured hydrophone output voltage versus frequency, illustrating a typical oscillating interference pattern resulting from a surface reflection. Solid line is measured sum of direct and reflected signals. Dashed line is computed direct signal.

¹ This formula is applicable to many types of interference. If standing waves are set up between two plane and parallel transducers, Δd is twice the distance between transducers. If "cross talk," or the interference between the direct acoustic signal and a purely electromagnetic signal, is present, Δd is the distance between transducers.

where Δf is the frequency interval between adjacent peaks or adjacent nulls, c is the speed of sound, and Δd is the path difference between the direct and the surface reflected signals. Figure 1 is a decibel or logarithmic plot. On a linear plot the oscillating pattern would have an approximately sinusoidal shape. In either case, the correct level of the direct signal is easily ascertained from the maxima and minima levels of the oscillations.

At audio frequencies the interference is not so simple. Figure 2 is an example of a hydrophone output voltage versus frequency. The sound projector was a USRL type J9 which has a smooth and almost constant transmitting response.² The hydrophone was a Massa type M115B, which has a constant receiving sensitivity. The 1.8 ratio of transducer separation to water depth was chosen to show the effect of interference in some detail; it is not the minimum ratio used at the USRL.

The interference oscillations appear to be inconsistent; they are of irregular shape and the amplitude is much greater than can be accounted for by a single surface or bottom reflection. The oscillations do, however, repeat at the same frequency interval Δf as would a single surface reflection.

Because of the long wavelengths at audio frequencies, directional transducers are not feasible. Short projector-

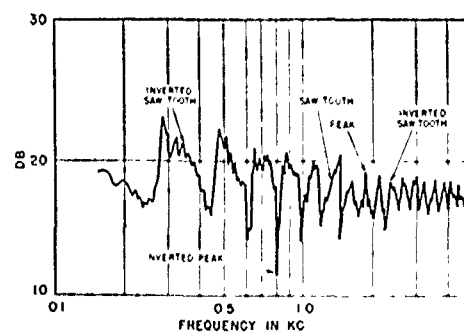


FIG. 2. Measured hydrophone output voltage where projector and hydrophone are both at a depth midway between the water-air surface and bubble covered bottom. The transducers are separated by a distance equal to $\frac{1}{4}$ of the water depth. The projector transmitting response and hydrophone receiving sensitivity are both essentially constant with frequency.

² C. C. Sims, Proc. Inst. Radio Engrs. 47, 866 (1959).

Interference Versus Frequency in Measurements in a Shallow Lake

ROBERT J. BOBBER

U. S. Navy Underwater Sound Reference Laboratory, Orlando, Florida

(Received March 22, 1961)

When an omnidirectional projector and hydrophone are closely spaced and in shallow water, and sound is transmitted from one to the other, a large interference signal is superimposed on the direct signal. If the received signal is plotted as a function of frequency, as in a calibration measurement, the interference signal amplitude appears to be an inconsistent series of irregular sharp peaks and dips. A mathematical analysis of the condition where the transducers are midway between a water-air surface and a bubble-covered bottom shows that the shape, amplitude, and frequency of the interference pattern are predictable as the result of a large number of multireflection paths.

INTRODUCTION

ACOUSTICAL measurements, particularly for the calibration of underwater sound transducers, are often made in shallow water. For economic or other practical reasons the absence of good free-field conditions must be tolerated.

The Underwater Sound Reference Laboratory calibrates transducers in a lake 25 to 30 ft deep. This depth is ample for measurements at ultrasonic frequencies because measurement transducers can be made directional to avoid difficulties with reflections from the top and bottom boundaries. Surface-reflected sound in the direction of minor lobes of the radiation pattern, and other types of interference, are easily recognized and accounted for. For example, Fig. 1 is a trace of a hydrophone output voltage versus frequency. The solid line is the measured voltage. The dashed line is the corrected voltage. The oscillating pattern can be identified as surface reflection interference from¹

$$\Delta f = c/\Delta d, \quad (1)$$

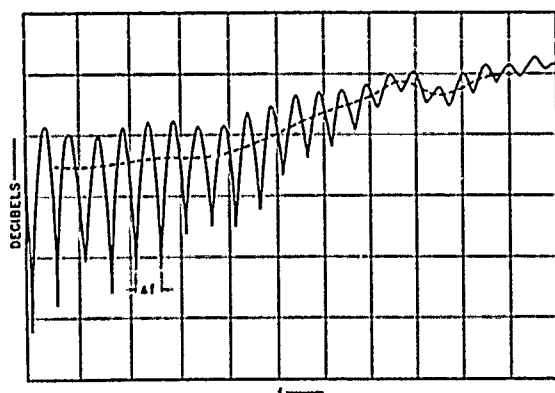


FIG. 1. Measured hydrophone output voltage versus frequency, illustrating a typical oscillating interference pattern resulting from a surface reflection. Solid line is measured sum of direct and reflected signals. Dashed line is computed direct signal.

¹ This formula is applicable to many types of interference. If standing waves are set up between two plane and parallel transducers, Δd is twice the distance between transducers. If "cross talk," or the interference between the direct acoustic signal and a purely electromagnetic signal, is present, Δd is the distance between transducers.

where Δf is the frequency interval between adjacent peaks or adjacent nulls, c is the speed of sound, and Δd is the path difference between the direct and the surface reflected signals. Figure 1 is a decibel or logarithmic plot. On a linear plot the oscillating pattern would have an approximately sinusoidal shape. In either case, the correct level of the direct signal is easily ascertained from the maxima and minima levels of the oscillations.

At audio frequencies the interference is not so simple. Figure 2 is an example of a hydrophone output voltage versus frequency. The sound projector was a USRL type J9 which has a smooth and almost constant transmitting response.² The hydrophone was a Massa type M115B, which has a constant receiving sensitivity. The 1:8 ratio of transducer separation to water depth was chosen to show the effect of interference in some detail; it is not the minimum ratio used at the USRL.

The interference oscillations appear to be inconsistent; they are of irregular shape and the amplitude is much greater than can be accounted for by a single surface or bottom reflection. The oscillations do, however, repeat at the same frequency interval Δf as would a single surface reflection.

Because of the long wavelengths at audio frequencies, directional transducers are not feasible. Short projector-

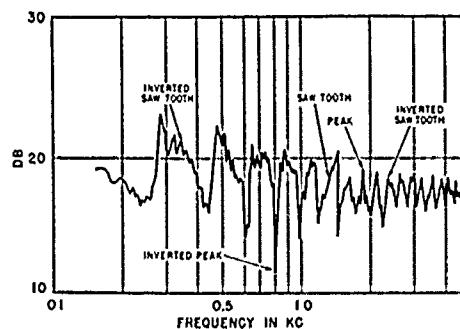


FIG. 2. Measured hydrophone output voltage where projector and hydrophone are both at a depth midway between the water-air surface and bubble-covered bottom. The transducers are separated by a distance equal to $\frac{1}{8}$ of the water depth. The projector transmitting response and hydrophone receiving sensitivity are both essentially constant with frequency.

² C. C. Sims, Proc. Inst. Radio Engrs. 47, 866 (1959).

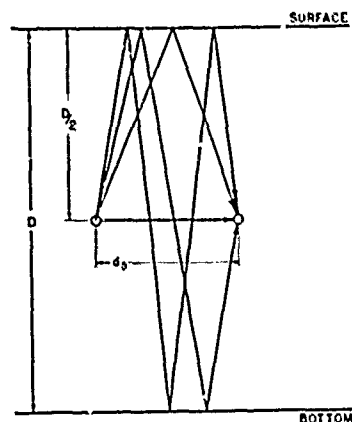


FIG. 3. Schematic drawing of assumed conditions for a projector and hydrophone in water. Paths are shown for the direct signal and for the single-double, and triple-reflection paths when the first reflection is from the surface.

to-hydrophone distances help to reduce the interference by increasing the ratio of direct-to-interfering signal amplitudes. It would appear helpful also to work as far away as possible from the nearest boundaries, or to work at a depth midway between surface and bottom. If the bottom happens to be a pressure release surface, as it frequently is because of gas bubbles from decaying organic matter,^{3,4} the mid-depth may be the worst place to work.

It will be shown that there is a regularity to the interference pattern shown in Fig. 2, and that the regularity, shape, and amplitude of the interference oscillations can be predicted as a result of placing two omnidirectional transducers midway between two water-air surfaces.

THEORY

Consider the condition shown in Fig. 3 where a projector and hydrophone are separated by a distance d_0 . The water depth is D , and both transducers are at the depth $D/2$. The depth is much larger than the distance d_0 . Both transducers are omnidirectional. Both surface and bottom are pressure release surfaces.

There is an infinite number of possible ray paths between the transducers. The direct path and paths involving 1, 2, and 3 reflections are shown in Fig. 3. For each number of reflections there are actually 2 paths, 1 for the first reflection at the surface and 1 for the first reflection at the bottom; only the surface-first paths are shown in Fig. 3.

The signal received by the hydrophone via the direct path is given by $A_0 \cos(\omega t - kd_0)$, where A_0 is the amplitude, ω is $2\pi f$ or angular frequency, t is time, and k is $2\pi/\lambda$ or ω/c or the wave number, λ is wavelength, c is the speed of sound in water.

The signal received by the hydrophone via the one-reflection path is given by $A_1 \cos(\omega t - kd_1 - \pi)$ where A_1 is the amplitude and d_1 the one-reflection path distance. The expression includes π because the signal

undergoes a phase reversal at each pressure-release boundary. Similarly, the signal from the two-reflection path is $A_2 \cos(\omega t - kd_2 - 2\pi)$, or from the n -reflection path is $A_n \cos(\omega t - kd_n - n\pi)$. The reflection path distances are given by

$$\begin{aligned} d_1 &= 2[(d_0/2)^2 + (D/2)^2]^{1/2}, \\ d_2 &= 4[(d_0/4)^2 + (D/2)^2]^{1/2}, \\ &\dots \dots \dots \\ d_n &= 2n[(d_0/2n)^2 + (D/2)^2]^{1/2}. \end{aligned}$$

Since $D \gg d_0$, the $d_0/2n$ term can be neglected, and the distances reduce to

$$\begin{aligned} d_1 &= D \\ d_2 &= 2D \\ &\dots \dots \dots \\ d_n &= nD. \end{aligned}$$

The amplitudes of the reflected signals can all be given in terms of the path lengths and the amplitude A_1

$$A_n = (d_1/d_n) \cdot A_1 = A_1/n.$$

If $2n[(d_0/2n)^2 + (D/2)^2]^{1/2} - nD \ll \lambda$, then the phase of the reflected signals can also be given in terms of the approximation $d_n \approx nD$ and the expressions for the reflected signals then become

$$\begin{aligned} &A_1 \cos(\omega t - kD - \pi), \\ &(A_1/2) \cos(\omega t - 2kD - 2\pi), \\ &\dots \dots \dots \\ &(A_1/n) \cos(\omega t - nkD - n\pi). \end{aligned}$$

The total signal H received by the hydrophone will be the sum of the direct and all reflected signals

$$H = A_0 \cos(\omega t - kd_0) + \sum_{n=1}^{\infty} (A_1/n) \cos(\omega t - nkD - n\pi).$$

The second term can be expanded as follows:

$$\begin{aligned} &\sum_{n=1}^{\infty} (A_1/n) \cos(\omega t - nkD - n\pi) \\ &= \sum_{n=1}^{\infty} (A_1/n) [\cos \omega t \cos(nkD + n\pi) \\ &\quad + \sin \omega t \sin(nkD + n\pi)]. \end{aligned}$$

Then

$$\begin{aligned} H &= A_0 \cos(\omega t - kd_0) \\ &+ [A_1 \sum_{n=1}^{\infty} n^{-1} \cos(nkD + n\pi)] \cos \omega t \\ &+ [A_1 \sum_{n=1}^{\infty} n^{-1} \sin(nkD + n\pi)] \sin \omega t. \end{aligned} \quad (2)$$

³ J. L. Jones, C. B. Leslie, and L. Barton, J. Acoust. Soc. Am. 30, 142 (1958).

⁴ R. J. Bobber, J. Acoust. Soc. Am. 31, 250 (1959).

If the substitutions

$$\cos(nkD + n\pi) = (-1)^n \cos(nkD)$$

$$\sin(nkD + n\pi) = (-1)^n \sin(nkD)$$

are made, Eq. (2) can be written

$$\begin{aligned} H = & A_0 \cos(\omega t - kd_0) \\ & + [A_1 \sum_{n=1}^{\infty} (-1)^n n^{-1} \cos nkD] \cos \omega t \\ & + [A_1 \sum_{n=1}^{\infty} (-1)^n n^{-1} \sin nkD] \sin \omega t. \end{aligned} \quad (3)$$

The total signal then is the sum of the direct signal and two reflection or interference components. The two interference components, given by the second and third terms in Eq. (3), are 90° out of phase with each other, and the phase of both with respect to the direct signal depends on the angle kd_0 . Since the direct path d_0 is much shorter than the one-reflection path D , the amplitude A_0 is much larger than the amplitude given by either bracketed term in Eq. (3). Therefore, an interference component which is in phase or 180° out of phase with the direct signal will add arithmetically to the direct signal, but an interference component which is 90° or 270° out of phase with the direct signal will have negligible effect on the amplitude of the total signal—that is,

$$|H| = A_0 \pm \left[A_1 \sum_{n=1}^{\infty} (-1)^n n^{-1} \frac{\cos nkD}{\sin nkD} \right] \quad (0^\circ \text{ or } 180^\circ \text{ phase difference})$$

$$|H| = \left\{ A_0^2 \pm \left[A_1 \sum_{n=1}^{\infty} (-1)^n n^{-1} \frac{\cos nkD}{\sin nkD} \right]^2 \right\}^{1/2} \approx A_0 \quad (90^\circ \text{ or } 270^\circ \text{ phase difference}).$$

The relative phase of the interference components and the direct signal will change continuously as a function of kd or frequency. Consider four conditions for d_0 given in wavelengths λ :

- (a) $d_0 = \lambda/4, 5\lambda/4, 9\lambda/4, \dots$ etc.
then $kd_0 = \pi/2$ and $\cos(\omega t - kd_0) = \sin \omega t$,
- (b) $d_0 = \lambda/2, 3\lambda/2, 5\lambda/2, \dots$ etc.
then $kd_0 = \pi$ and $\cos(\omega t - kd_0) = -\cos \omega t$,
- (c) $d_0 = 3\lambda/4, 7\lambda/4, 11\lambda/4, \dots$ etc.
then $kd_0 = 3\pi/2$ and $\cos(\omega t - kd_0) = -\sin \omega t$,
- (d) $d_0 = 0, \lambda, 2\lambda, \dots$ etc.
then $kd_0 = 0$ and $\cos(\omega t - kd_0) = \cos \omega t$.

For conditions (a) and (c), the sine component, or the third term in Eq. (3), will have a 0° or 180° phase relation with the direct signal. The cosine component,

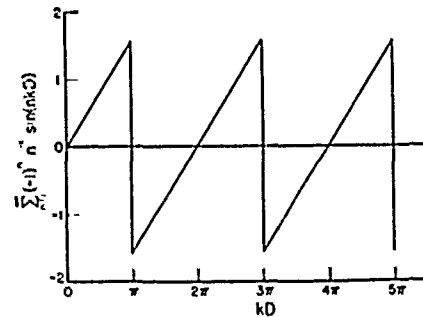


Fig. 4. Saw-tooth component of received signal as a function of wave number times depth (kD).

or the second term in Eq. (3), will have a 90° or 270° phase relation with the direct signal and can be neglected. Equation (3) then simplifies to

$$H = [\pm A_0 + A_1 \sum_{n=1}^{\infty} (-1)^n n^{-1} \sin nkD] \sin \omega t. \quad (4)$$

For conditions (b) and (d), the cosine component will have 0° or 180° phase relation with the direct signal. The sine component will have a 90° or 270° phase relation with the direct signal and can be neglected. Equation (3) then simplifies to

$$H = [\pm A_0 + A_1 \sum_{n=1}^{\infty} (-1)^n n^{-1} \cos nkD] \cos \omega t. \quad (5)$$

The summation term in Eq. (4) is the same as that for the Fourier series for an inverted⁵ saw-toothed wave.⁶ If it is plotted as a function of kD or frequency, the saw-toothed interference wave in Fig. 4 is obtained. The term "wave" here applies to a periodic variable as a function of frequency rather than of time or distance as is the usual case, and will be referred to as an "interference wave" when necessary to distinguish it from the real acoustic wave. Where A_0 and A_1 have opposite signs, the inverted saw-toothed wave is inverted again, and a normal or positive⁵ saw-toothed wave is obtained.

The summation term in Eq. (5) is, in spite of its simple form, not commonly used and not found in the usual references on Fourier series or wave forms. A plot of the sum of the first five terms is shown in Fig. 5. This interference wave shape will be referred to as a peak wave in the form shown, or when A_0 and A_1 have the same sign, and as an inverted peak wave in the negative sense, or when A_0 and A_1 have opposite signs. Of special significance is the amplitude of the sharp peak. When $kD = \pi, 3\pi, 5\pi$, etc., the summation

⁵ As used here, a positive or normal saw-toothed wave has a slant line with a positive slope. A negative or inverted saw toothed wave has a slant line with a negative slope.

⁶ F. E. Terman, *Radio Engineers' Handbook* (McGraw Hill Book Company, Inc., New York, 1943), pp. 21-22.

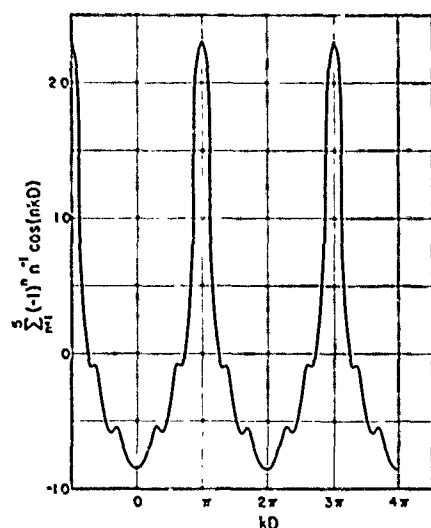


FIG. 5. Sum of first five terms of expression for the peaked component of received signal as a function of wave number times depth (kD)

term in Eq. (5) or cosine series becomes

$$1 + 1/2 + 1/3 + 1/4 + \dots + 1/n.$$

This is a harmonic series which is divergent. Thus, the amplitude of the sharp peak increases without limit as n increases. The negative amplitude is the sum of $-1 + 1/2 - 1/3 + 1/4 - \dots$ which converges to $-\ln 2$ or approximately -0.69 .

The terms in parentheses in Eqs. (4) and (5) describe the amplitude of the total acoustic signal under four different conditions. Since A_0 and A_1 are almost constants with frequency, the shapes of these amplitude functions, or interference waves, when kD or frequency is a variable, are described by the summation terms.

Table I summarizes the relations among the four conditions, the form of Eqs. (4) or (5) which applies, and the wave shape of the amplitude. Consequently, for the conditions assumed in this analysis, the amplitude wave shape should change from inverted saw-tooth to inverted peak to saw-tooth to peak, and then through the same sequence again, as the frequency is increased.

The frequencies at which each wave shape will appear are calculated from the d_0/λ ratios. The inverted saw-toothed wave, for example, will appear when

$$d_0 = \lambda/4 = c/(4f)$$

or

$$f = (1/4)(c/d_0). \quad (6)$$

Similarly, the inverted peak wave will appear when $f = (1/2)(c/d_0)$, the saw-toothed wave when $f = (3/4)(c/d_0)$, and the peak wave when $f = c/d_0$. At intermediate frequencies, the wave shape will, of course, be a complex combination of saw-toothed and peak waves.

The amplitude for the saw-toothed wave when $n \rightarrow \infty$ is $\pm 1.57 A_1$, and for the peak wave is $+\infty$ and $-0.69 A_1$.

The ratio of A_1/A_0 for a single boundary reflection would be d_0/D ; however, the amplitude A_1 is the sum of one surface and one bottom reflection. Therefore, $A_1 = 2.1 d_0/D$, and the maximum amplitude of the interference waves becomes $\pm 1.57(2.1 d_0/D)$ for the saw-toothed wave, and $+\infty$ and $-0.69(2.1 d_0/D)$ for the peak wave.

On a decibel scale, the interference wave amplitude is given by

$$\left. \begin{aligned} &+20 \log(1 + 3.14 d_0/D) \\ &-20 \log(1 - 3.14 d_0/D) \end{aligned} \right\} \text{(saw-tooth)}$$

$$\left. \begin{aligned} &+\infty \\ &-20 \log(1 - 1.38 d_0/D) \end{aligned} \right\} \text{(peak)}.$$

For a typical ratio $d_0/D = 0.12$, these amplitudes become $+2.8$ and -4.1 db for the saw-toothed wave, and $+\infty$ and -1.6 db for the peak wave. For similar amplitudes resulting from a single reflection from a single boundary the values are ± 1.0 db.

DATA AND DISCUSSION

The interference waves in the curve in Fig. 2 clearly show the sequence of shapes predicted by the theory.

At frequencies of 300 to 500 cps, the peak-to-peak amplitudes of the saw-toothed waves are approximately 7 db—again in good agreement with theory. At higher frequencies, the assumption of omnidirectional transducers loses validity. The effect of a directional transducer is to reduce the ratio of A_1/A_0 and of the interference wave amplitude. It does not affect the wave shape.

The top and bottom boundaries in any practical situation are not perfect reflectors and some energy is lost through both boundaries. Because of this energy loss and the absence of other ideal conditions, the number of reflection paths effective in forming the interference waves is limited. Clues to how many reflection paths are effective are available in the number of secondary oscillations on the saw-toothed wave and the amplitude of the peak wave.

Analysis of data obtained when d_0/D is 0.10 to 0.12 indicates that 20 to 30 reflections are effective in forming the interference waves—a surprisingly large number.

It was assumed in the theory that d_n was approximately equal to nD . The errors in this assumption are largest for $n=1$ or the first reflection and at the highest frequencies. For $d_0=100$ cm and $D=800$ cm, the distance or magnitude error for $n=1$ is 7 cm or less than 1 percent. The phase error is 33.6° at 2 kc and 8.4° at 500 cps. The phase error is obviously the more important of the 2, and along with the directivity, is responsible for degeneration of the interference pattern at high audio frequencies.

TABLE I. Summary of interference wave shape analysis.

Condition	Total signal amplitude	Amplitude wave shape
$d_0 = \lambda/4, 5\lambda/4, \text{etc.}$	$+A_0 + A_1 \sum_{n=1}^{\infty} (-1)^n n^{-1} \sin n k D$	Inverted saw-tooth
$d_0 = \lambda/2, 3\lambda/2, \text{etc.}$	$-A_0 + A_1 \sum_{n=1}^{\infty} (-1)^n n^{-1} \cos n k D$	Inverted peak
$d_0 = 3\lambda/4, 7\lambda/4, \text{etc.}$	$-A_0 + A_1 \sum_{n=1}^{\infty} (-1)^n n^{-1} \sin n k D$	Saw-tooth
$d_0 = 0, \lambda, 2\lambda, \text{etc.}$	$+A_0 + A_1 \sum_{n=1}^{\infty} (-1)^n n^{-1} \cos n k D$	Peak

The four types of interference waves appear at frequencies very close to those predicted by Eq. (6) and theory. A small, but consistent and unexplained, discrepancy can be noticed at the higher frequencies. The peak wave in Fig. 2, for example, appears at 1.5 to 1.9 kc, where the computed value ($f = c/d_0$) is 1.525 kc.

OTHER BOUNDARY CONDITIONS

With a single plane boundary such as the water-air surface, the total signal is the sum of the direct signal and one reflection

$$H = B_0 \cos(\omega t) + B_1 \cos(\omega t + \theta),$$

where B_0 and B_1 are the amplitudes of the direct and reflected signal and θ is the phase difference between them. This expression can be expanded and rearranged

$$H = B_0 \cos \omega t + B_1 [\cos \omega t \cos \theta - \sin \omega t \sin \theta],$$

$$= (B_0 + B_1 \cos \theta) \cos \omega t - (B_1 \sin \theta) \sin \omega t.$$

If $B_0 \gg B_1$, the second term can be neglected and

$$H = (B_0 + B_1 \cos \theta) \cos \omega t.$$

The amplitude $(B_0 + B_1 \cos \theta)$ will oscillate as a function of θ and will repeat when

$$\theta = 2n\pi$$

or

$$2\pi \Delta d / \lambda = 2n\pi,$$

where n is an integer and Δd is the difference in path length between the direct and reflected signal. Then

$$\Delta d = n\lambda = c/f,$$

$$f = nc / \Delta d,$$

or

$$\Delta f = c / \Delta d, \quad (7)$$

where Δf is the repetition frequency or frequency difference between adjacent interference peaks. Equation (7) is the same as Eq. (1).

Under some practical conditions, particularly in air acoustics, the top and bottom boundaries may both be rigid instead of pressure release—a large, low-ceilinged room with hard floors and ceilings, for example. It can be shown that these boundary conditions merely eliminate the $(-1)^n$ terms in Eq. (3), and that this results in a shift of π in the interference waves—that is, in Figs. 4 and 5, the $0, 2\pi, 4\pi, \text{etc.}$, points on the abscissa would be shifted by π in either direction. Otherwise, the rigid boundary condition is the same as the pressure-release condition.

An implication of the theory is that when one boundary is rigid and the other is pressure release, the interference at points midway between will completely cancel. Attempts have been made to test this aspect of the theory. The results were inconclusive because of the practical difficulty of obtaining a large or widespread, rigid, bottom boundary in water.

Working at a depth shallower or deeper than the mid-depth does not eliminate the interference problem, it merely complicates the analysis of the situation. However, because of the symmetrical boundary conditions, the maximum coherence of the many interfering signals and therefore maximum interference would be expected at mid-depth.

CONCLUSION

Where an omnidirectional projector and hydrophone are closely spaced in shallow water, the acoustical interference measured as a function of frequency can be explained on the basis of a large number of multi-reflected sound rays. When the transducers are half way between the water-air surface and a bubble pressure-release bottom, the true frequency response curve has superimposed upon it an interference pattern which is a sequence of saw-tooth and peak wave shapes. For a projector-to-hydrophone distance equal to one-tenth to one-eighth of the total water depth, the interference wave shapes can be expected to have amplitudes of 7 to 8 db.

Section	<input checked="" type="checkbox"/>
Use	<input type="checkbox"/>
	<input type="checkbox"/>

COPIES
SPECIAL

A 20